Regional CO_2 and Latent Heat Surface Fluxes in the Southern Great Plains: Measurements, Modeling, and Scaling

W.J. Riley, S.C. Biraud, M.S. Torn, M.L. Fischer, D.P. Billesbach, J.A. Berry

Key words: agricultural systems; biogeochemical cycles, processes, and modeling; biosphere/atmosphere interactions; carbon cycling; biogeochemical cycles, processes, and modeling

Abstract

Characterizing net ecosystem exchanges of CO_2 (NEE) and sensible and latent heat fluxes in heterogeneous landscapes is difficult, yet critical given expected changes in climate and land use. We report here a measurement and modeling study designed to improve our understanding of surface to atmosphere gas exchanges under very heterogeneous land cover in the mostly agricultural U.S. Southern Great Plains (SGP). We combined three years of site-level, eddy-covariance measurements in several of the dominant land-cover types with regional-scale climate data from the distributed Mesonet sampling stations and NEXRAD precipitation measurements to calibrate a land-surface model of trace-gas and energy exchanges (ISOLSM). Yearly variations in vegetation cover distributions were estimated from MODIS NDVI and compared to regional and sub-regional vegetation cover type estimates from the USDA census. We first applied ISOLSM at a 250 m spatial scale to account for vegetation cover type and leaf area variations that occur on hundred meter scales. Because of computational constraints, we developed a sub-sampling scheme within 10 km 'macrocells' to perform these high-resolution simulations. We estimate that the Atmospheric Radiation Measurement Climate Research Facility (ACRF) SGP region net CO_2 exchange with the local atmosphere was -240, -340, and -270 gC m^{-2} y^{-1} (positive toward the atmosphere) in 2003, 2004, and 2005, respectively, with large seasonal variations. We also performed simulations using two scaling approaches at resolutions of 10, 30, 60, and 90 km. The scaling approach applied in current land-surface models led to regional NEE biases of up to 50 and 20% in weekly and annual estimates, respectively. An important factor in causing these biases was the complex LAI distribution

within cover types. Biases in predicted weekly-average regional latent heat fluxes were smaller than for NEE, but larger than for either ecosystem respiration or assimilation alone. However, spatial and diurnal variations of hundreds of W m^{-2} in LH fluxes were common. We conclud that, in this heterogeneous system, characterizing vegetation cover type and LAI at the scale of spatial variation are necessary for accurate estimates of bottom-up, regional NEE and surface energy fluxes.

Introduction

Accurately quantifying terrestrial carbon (C) exchange with the atmosphere is critical for estimates of anthropogenic impacts on climate [*IPCC*, 2007], terrestrial C sequestration potential [*Bachelet et al.*, 2001], and dynamic vegetation changes under climate change [*Lenihan et al.*, 2003]. Gross terrestrial C exchanges (i.e., assimilation and respiration) with the atmosphere are more than ten times larger than current anthropogenic fossil fuel CO_2 emissions [*Raupach et al.*, 2007], implying that small errors in terrestrial exchange estimates can result in relatively large errors in predicted atmospheric CO_2 levels.

There are a number of approaches to estimating terrestrial C exchanges: (1) 'bottom-up' approaches using spatial scaling with distributed surface flux measurements [*Desai et al.*, 2008] or forest and agricultural inventories; (2) bottom-up approaches that attempt to mechanistically model the various processes producing and consuming CO_2; (3) 'top-down', or inverse, approaches that use atmospheric concentration measurements, atmospheric transport fields, and (in some cases) *a priori* surface exchange estimates; and (4) estimates based on remotely-sensed properties of the land surface. The many examples of these approaches span a large range of mechanistic detail, temporal and spatial resolution, and extent of testing and comparison with independent measurements.

Many "bottom-up" models have been developed to integrate the processes responsible for gross and net terrestrial C exchanges and their relationships with climate (e.g., [*Bonan*, 1996; *Bonan et al.*, 2002; *Dickinson et al.*, 1986; *Gu et al.*, 2002; *Parton et al.*, 1988; *Potter et al.*, 1993; *Running and Hunt*, 1993; *Sellers et al.*, 1986]). These models span a large range of integration of mechanistic understanding, from simple regression models based on local climate to complex representations of molecular-level exchanges. Model testing has typically been performed using field-scale observations from, for example, soil respiration chamber and eddy

covariance measurements. There have also been models developed specifically for cropped systems, including DSSAT [*Jones et al.*, 2003] and Agro-IBIS [*Kucharik and Twine*, 2007]. Some of these land-surface models have been integrated in regional (e.g., [*Kueppers et al.*, 2007; *Riley et al.*, 2005; *Wang et al.*, 2007]) and global [*Collins et al.*, 2006] climate models. However, there remains a substantial gap between the scales at which these models are applied and the scales at which they were developed and tested. An important concern in bottom-up model applications is how surface heterogeneity in land cover type and status is taken into account, since in many systems these parameters vary on smaller spatial scales than can be accounted for with the model [*Jarvis*, 1995]. A number of studies have addressed spatial scaling issues, primarily in natural or forested systems [*Chen et al.*, 2007; *Kimball et al.*, 1999; *Li et al.*, 2008; *Turner et al.*, 2000]. However, to our knowledge, no comparable spatial scaling analysis has been performed for a predominantly agricultural landscape.

Inverse, or top-down, approaches infer surface C exchanges from atmospheric measurements and tend to focus on large spatial scales, from regional [*Bakwin et al.*, 2004; *Helliker et al.*, 2004; *Lin et al.*, 2004; *Wang et al.*, 2007; *Williams et al.*, 2005] to global [*Chevallier et al.*, 2005; *Deng et al.*, 2007; *Gurney et al.*, 2003; *Lokupitiya et al.*, 2008; *Peters et al.*, 2007; *Rodenbeck et al.*, 2003; *Stephens et al.*, 2007]. A common thread in these models is the need for land-surface models with readily adjustable parameters that can be optimized based on comparison of predicted and measured atmospheric mixing ratios. Because many inverse approaches include consideration of multiple sources of uncertainty [*Gerbig et al.*, 2003], identifying likely uncertainties in the land surface parameterizations for ecosystem fluxes is of significant interest and importance.

Remotely-sensed estimates of terrestrial gross primary production (GPP) have been developed, for example, using MODIS satellite optical and near-infrared spectral wavelengths [*Field et al.*, 1998; *Goetz et al.*, 1999; *Nemani et al.*, 2003; *Prince and Goward*, 1995; *Zhao et al.*, 2005]. A number of studies have compared MODIS-based GPP estimates with GPP inferred from eddy covariance measurements, primarily in forested systems and secondarily in grasslands [*Coops et al.*, 2007; *Heinsch et al.*, 2006; *Turner et al.*, 2004; *Turner et al.*, 2006; *Zhang et al.*, 2007].

Currently, the methods described above all have shortcomings when applied to estimating C budgets of complex, spatially heterogeneous regions. In fact, even determining whether a

particular modeling approach is accurate in such a system is difficult, since one cannot directly monitor the C exchanges across a large region with varying cover types and vegetation status. On the other hand, accurately estimating these C exchanges is critical to improve climate prediction, for climate change attribution, and to account for the costs of fossil fuel CO_2 emissions [*Stern*, 2006].

In this study we developed and applied a bottom-up, distributed, land-surface modeling approach in a very heterogeneous region (Atmospheric Radiation Measurement (ARM) Climate Research Facility (ACRF)) in the U.S. Southern Great Plains to estimate terrestrial C exchanges at spatial scales consistent with the scale of vegetation heterogeneity. The ACRF comprises about 300×400 km in Oklahoma and Kansas, and is very well instrumented for the study of atmospheric radiation, clouds, land-surface exchanges, and their interactions. The area is largely agricultural and is spatially and temporally heterogeneous in vegetation cover type and status (Figure 1). Measurements distributed in the facility include a 60 m tower instrumented with eddy covariance systems measuring CO_2, latent heat (LH), and sensible heat (SH) fluxes at 4, 25, and 60 m; two portable eddy covariance systems; atmospheric and cloud sensing systems; and regular balloon sonde and aircraft measurements. Meteorological forcing data are available from the Kansas and Oklahoma Mesonet sites [*Brock et al.*, 1995]. For this analysis, we tested and used a previously described method [*Doran et al.*, 1998] to estimate climate forcing from the OK and KS Mesonet datasets. Surface cover type was estimated at 250 m resolution from satellite NDVI data and archetypal annual NDVI profiles and compared to county-level statistics. We then calibrated and tested a land-surface model (ISOLSM [*Riley et al.*, 2002]) using eddy covariance data from three of the dominant land use types.

We applied these measurements and modeling tools to characterize the region's net surface C (NEE) and energy exchanges with the local atmosphere for three years (2003 – 2005). We note that NEE estimates in agricultural systems do not represent a 'true' atmospheric sink, since much of the agricultural product is shipped out of the region, where it may be returned to the atmosphere relatively quickly. Our objectives were to understand how spatial and temporal variability in cover type and status affect regional exchanges and to quantify uncertainty in NEE and latent heat flux estimates resulting from spatial resolution in surface characterization and forcing variable estimates. These three years spanned large variations in the amount and spatial distribution of precipitation, and we therefore expected substantial inter-annual variability in

regional NEE and surface energy exchanges. We also expected that the spatial resolution at which vegetation cover type and status are specified would affect regional NEE and surface energy exchange estimates.

Methods

Meteorological Forcing

We created a spatially and temporally distributed meteorological forcing dataset from the Oklahoma and Kansas Mesonet datasets [*Brock et al.*, 1995]. The Oklahoma and Kansas Mesonet consists of ~139 platforms distributed throughout the two states. Stations in and immediately surrounding the ACRF are shown in Figure 2. Each station measures relative humidity, wind speed, air temperature and pressure, and downward solar radiation, and reports these data as five, thirty, or sixty-minute averages. The ARM archive (www.arm.gov, [*Ackerman et al.*, 2004]) makes these data available a few days after the measurements are collected. We estimated downward infrared radiation using Boltzman's law, observed air temperature, and estimates of surface and atmospheric emissivity.

We distributed the atmospheric forcing data required by ISOLSM to a user-defined resolution using the approach of Doran et al. [1998]. For the results presented below, we use several grid resolutions (i.e., 10, 30, 60, and 90 km) for the interpolated atmospheric forcing. Because of the spacing between Mesonet sites (~15 km), resolutions finer than about 10 km do not add more information to the interpolated field.

We calculated the weighting factors, α_i, using:

$$H(x) = \sum_{i=1}^{N} \alpha_i Q(x - x_i). \quad (1)$$

Here, $H(x)$ is the interpolated meteorological field, $Q(x\text{-}x_i)$ is a radial basis function, and x_i is the distance to a particular observation point. The basis function is calculated as:

$$Q(x - x_i) = \sqrt{\frac{(x - x_i)^2}{c^2} + 1}, \quad (2)$$

where c is a smoothing parameter (taken as 0.05). Finally, the interpolated meteorological field, H_{ip}, is calculated as:

$$H_{ip} = Q_g \alpha, \quad (3)$$

where Q_g and α are matrices formed from Q and α_i. After interpolation, we performed checks on the interpolated fields to ensure that all values at all times and spatial points were within reasonable ranges.

Hourly precipitation estimates at 4 km resolution were generated using NEXRAD radar precipitation [*Fulton et al.*, 1998] and rain gauge reports over the Arkansas Red river basin. This dataset is available on the ARM archive; we spatially regridded the hourly data to the user-defined spatial resolution.

Estimating Surface Cover Type and LAI from MODIS NDVI

To estimate surface cover type and LAI (L, m^2 m^{-2}) across the ACRF we used the 250 m NDVI (N (-)) product (http://lpdaac.usgs.gov/modis/dataproducts.asp#mod13). Because cover type and LAI vary across the ACRF on 100 m scales, a continuous finer resolution product would be preferable; however, such temporally- and spatially-resolved observations are currently unavailable. The NDVI product is produced every sixteen days from daily 250 m MODIS red and near infrared surface reflectance data. The composites are based on the maximum NDVI for the compositing period, and the data are provided as an Alber's Conic Equal Area projection.

We determine the surface cover type by convolving an archetypal normalized NDVI history, N_i, for each vegetation type with the satellite-derived estimate of NDVI (N):

$$Z(v) = \frac{\int_0^1 N_i(v) N dt}{\int_0^1 N_i(v) dt}. \quad (4)$$

Here, v is the vegetation type (-); Z is the ranking index for each vegetation type (-); and t is time (y). Note that we have normalized the archetypal NDVI histories to ensure that variations and uncertainties in the peak magnitudes of N do not affect the ranking index. The archetypal histories were derived from LAI observations in the ACRF using the method described in Sellers et al. [1996]. The vegetation type for each 250 m pixel is determined by the highest value of Z calculated for the full year. This approach did not adequately separate summer C_4 crops from pastures, which are a mixture of C_3 and C_4 grasses. Therefore, at the end of the process, C_4 crop cells with high N in April were set to be pasture because C_4 crops do not typically have appreciable LAI in April. Although crude, this method broadly captured the vegetation

distributions seen in the 2002 USDA Census data [*USDA*, 2002], as described below. Estimation of LAI from NDVI data can be problematic, particularly for high LAI and clumped vegetation. For this study, we mapped the five dominant vegetation types in the ACRF onto those described in Sellers et al. [1996], and used their approach to infer LAI.

Estimating Surface Cover Type from County-Level Data

For comparison to the vegetation type distributions estimated from MODIS NDVI, we estimated fractional cover for each vegetation type from county-level data contained in the 2002 Census of Agriculture [*USDA*, 2002]. This census is taken on a 5-year cycle, with farm data collected in years ending in 2 and 7. The census definition of a farm is any place from which $1,000 or more of agricultural products were produced and sold, or normally would have been sold, during the census year. The crop production data contained in the Census are collected for many cover types, so we consolidated the data to facilitate comparisons to the cover types simulated by ISOLSM (Table 1). Because the crop production data are for 2002, and planting of various crop types depends strongly on climatic and economic conditions and can have substantial interannual variability, we do not expect perfect agreement between the NDVI- and Census-derived fractions of land occupied by each cover type. However, agreement between the two methods for relative proportion of each land cover type within the region gave us some confidence that vegetation type is appropriately accounted for in the simulation results.

Eddy Covariance Flux Measurements

Eddy covariance fluxes were calculated using methods described in Billesbach et al. [2004] and Fischer et al. [2007]; we summarize them briefly here. The flux measurements have been made continuously since 2002 in one winter wheat field and for growing seasons up to the present in several additional fields (5 pastures, 4 winter wheat, and 3 sorghum) in the ACRF, with most of the measurements taking place near the Central Facility [*Fischer et al.*, 2007] (Figure 2). Each system is comprised of a sonic anemometer and an open-path infrared gas analyzer (IRGA; Li-COR Li-7500), a set of meteorological instruments that monitor net and photosynthetically active radiation, air temperature and relative humidity, precipitation, soil heat flux, and soil moisture and temperature (for more details, see Billesbach et al. [2004]). The IRGAs are calibrated before and after each deployment.

Fluxes were calculated on half-hour averages using standard algorithms comprising spike removal, coordinate rotation to zero mean vertical wind, and block averaging of scalar quantities. Density corrections [*Webb et al.*, 1980] were applied to the covariances of vertical wind with measured CO_2 and H_2O densities obtained with the IRGA. Fluxes were calculated by lagging the wind fluctuations in time to maximize the covariance (typical lag < 0.5 s). Multiplicative spectral corrections, caused by sensor separation and other factors [*Moore*, 1986], were calculated after confirming that the measured co-spectra were consistent with similarity theory. In general, the corrections were small (~10%), did not introduce systematic biases, were consistent across the different field sites, and hence were not applied to the data.

The eddy covariance fluxes were corrected for changes in CO_2 stored below the 4 m measurement height using measured CO_2 concentrations. An examination of subsets of the data showed that the storage corrections are small compared with turbulent fluxes except when friction velocity, u^*, is small.

From a total of 1732 site-days of deployment in 2002 - 2004, data passed quality control approximately 80% of daytime hours. Losses were mainly due to occasional photovoltaic power systems losses and bad IRGA signals during rain events. Nighttime data were subjected to a quality control on turbulence intensity as judged by friction velocity. Examination of selected datasets showed that nighttime NEE either did not vary significantly with u^* or increased to asymptotic values for u^* between 0.1 and 0.3 m s^{-1}. We subjected nighttime data to the constraint that $u^* > 0.1$ m s^{-1}, which passed 69% of nighttime data.

Land-Surface Model (ISOLSM)

For simulations presented here we used the land-surface model ISOLSM [*Aranibar et al.*, 2006; *Riley et al.*, 2002; *Riley et al.*, 2003], which is based on LSM1 [*Bonan*, 1996]. ISOLSM is a "big-leaf" (e.g., [*Dickinson et al.*, 1986; *Sellers, Randall et al.*, 1996]) land-surface model that simulates CO_2, H_2O, and energy fluxes between ecosystems and the atmosphere. ISOLSM simulates aboveground fluxes of radiation, momentum, sensible heat, and latent heat (L); vertically explicit energy and water fluxes below ground, and coupled CO_2 and H_2O exchange between soil, plants, and the atmosphere. Soil hydraulic characteristics are determined from soil sand, silt, and clay content and used in a Richard's equation approach to estimate soil moisutre. Soil C effluxes are estimated as the sum of autotrophic and heterotrophic respiration, with the

latter predicted using soil temperature (i.e., Q_{10} approach), moisture, and organic C content. The primary enhancements in ISOLSM (as compared to LSM1) relevant to this study include (1) modules that simulate the ecosystem isotopic stocks and exchanges of $H_2{}^{18}O$, HDO, $C^{18}OO$, and $^{13}CO_2$; (2) modification of the gross photosynthesis calculations, as described below; and (3) estimation of LAI and land cover type from satellite data. ISOLSM and LSM1 have been tested in a range of ecosystems at the site level (e.g., [*Bonan et al.*, 1995; *Bonan et al.*, 1997; *Riley et al.*, 2003]).

The version of ISOLSM applied here differs from that described in Riley et al. [2002] by several changes made to the plant physiology submodel. First, low and high temperature inhibition factors on the maximum catalytic capacity of Rubisco (V_m) from Sellers et al. [1996] have been included. Second, we implemented the method of Sellers et al. [1996] to smooth transitions between the three limiting assimilation rates (i.e., Rubisco, light, and export limited). Finally, iterations to estimate C_c and C_i, the leaf chloroplast and internal CO_2 concentrations, respectively, are now performed using net photosynthesis (i.e., accounting for leaf respiration occurring inside the leaf), as opposed to gross photosynthesis, as done in the original version of LSM1. Of these changes, the last had the largest impact, resulting in values for V_m and C_i that are much closer to measured values. We note, however, that we obtained similar GPP and NEE estimates with the two approaches. Although excluding leaf respiration from the photosynthesis iteration (in our old approach) did not degrade NEE estimates, the unrealistic C_i values obtained could be problematic when estimating isotopic fluxes (e.g., $^{13}CO_2$, $C^{18}OO$).

We added or modified five new land-surface types to ISOLSM corresponding to the dominant vegetation in the ACRF: summer C_3 crop, winter C_3 crop, summer C_4 crop, pasture (C_3 and C_4 grasses), and broadleaf deciduous forest. We estimated ecosystem parameters for these systems using the Mesonet meteorological forcing data and the eddy covariance measurements described above. ISOLSM was calibrated to the data for these land-surface types using an iterative least-squares fit for soil carbon content, C_s (kg C m^{-2}), and the maximum rate of carboxylation, V_m (μmol m^{-2} s^{-1}). The approach minimized differences between predicted and observed NEE during two periods: nighttime (9 PM – 4 AM) and daytime (10 AM – 2 PM). We first estimated C_s using nighttime data, since soil heterotrophic respiration continues during the day and must be subtracted from NEE in order to estimate V_m. The data available for the parameter generation and test of the resulting simulations are described in Table 2.

We modeled the pasture as a combination of C_3 and C_4 grasses, with leaf area indices for each type varying differently over the year. We applied the results of Still et al. [2003] to partition the NDVI-derived LAI into C_3 and C_4 components for each grid cell. They estimated that the C_4 percentage in April, June, July, and September is 38, 47, 50, and 85%, respectively. We used linear interpolation to estimate the C_4 percentage for the remaining months. Several features of cropped systems are not explicitly simulated in ISOLSM, including fertilizer and water application, planting and harvesting, and residue removal. We note that most of the ACRF is rainfed, so that water management should not be a large source of error, and that the observed LAI profiles should give relatively accurate estimates of when crops are planted and harvested. Forcing the model with observed LAI profiles should also somewhat mitigate inaccuracies resulting from the model's inability to predict the effects of fertilizer application on LAI and photosynthesis. Measuring fertilizer application rates, and accurately modeling their effects, at fine spatial scales across the ACRF would be difficult; however, such an effort should be considered in future work.

Simulations

The ACRF covers about 12,000 km^2. Therefore simulations at a spatial resolution of 250 m require about 2,000,000 cells to span the region. Simulating multiple years at this resolution across the ACRF was intractable given our computational resources. We devised the following sampling strategy to address this issue for the fine-resolution (i.e., 250 m) simulations. First, a uniform coarse grid (composed of 'macrocells') was superimposed across the region. For example, about 1200 macrocells measuring 10×10 km span the ACRF. Within each macrocell, we simulated up to ten randomly chosen 250 m grid cells (microcells) for each of the six possible vegetation covers present in region. Fewer than ten microcells may be present in a macrocell if a particular vegetation cover type is sparse in that macrocell. Macrocell land-surface fluxes for each vegetation cover type were calculated as a mean and standard deviation (SD) of the modeled microcell fluxes. This sampling approach substantially reduced the required simulation time while still providing land-surface flux mean and variability estimates from each vegetation cover type.

Spatial Scaling Simulations

We tested two methods, which have been applied in previous spatial scaling studies, for estimating regional CO_2 and LH fluxes at model resolutions greater than 250 m. The first, and simplest, approach was to perform the simulation with the dominant surface cover (i.e., corresponding to the largest fractional cover) and an average LAI computed from the cell. The second approach used the mean LAI for each surface cover type in the cell and weighted the results by the fractional cover of each cover type. This second method is applied, for example, in the NCAR GCM land-surface model CLM [*Dai et al.*, 2003]. We tested the accuracy of these approaches in estimating regional NEE and LH fluxes by consolidating climate forcing, LAI, and soil characterization at 10, 30, 60, and 90 km scales. For the climate forcing, the interpolation approach described above was performed at the user-specified resolution. The predicted regional NEE and LH fluxes using these methods was compared to those calculated at 250 m resolution.

Results and Discussion

Meteorological Forcing

We compared interpolated meteorological fields to measurements from the Mesonet sites (which were used in the interpolation) as well as to several sources not used in the interpolation: ARM Extended Facilities (EF, [*Ackerman et al.*, 2004]) observations and eddy covariance tower observations. An example of the climate forcing data calculated using the Mesonet and Extended Facilities data is shown in Figure 2 (surface relative humidity on March 22 2003 at 00:00). The interpolation method accurately reproduced the Mesonet measurements used in the interpolation; independent (not used in the interpolation) eddy covariance measurements over two continuous years in winter wheat and over the growing season in two pastures, three other winter wheat fields, and two sorghum fields (e.g., Figure 3); and independent observations from Extended Facilities stations (Table 4).

Typically, annual cumulative precipitation increases from East to West across the ACRF. Annual precipitation differed substantially among the three years (754, 950, and 797 mm in 2003, 2004, and 2005, respectively), with 2004 being the wettest year. Substantial inter-annual differences also occurred in the seasonality of precipitation.

In heterogeneous systems such as the ACRF, spatial variability in surface energy fluxes can cause heterogeneous near-surface winds, temperature, and humidity. There is a negative feedback on this climate forcing field heterogeneity, since the resulting increase in mixing will tend to homogenize these fields. This mixing can, to some extent, ameliorate this problem for modeling approaches that do not fully characterize the spatial variability of climate forcing within a computational domain. For this study, because the climate observations we used are spatially dense, our derived climate forcing likely captures the spatial variability actually experienced by individual points on the land-surface.

Surface Cover Type and LAI

We compared our surface cover type predictions to USDA county-level agricultural census statistics at three scales: (1) county, (2) the four quadrants of the ACRF, and (3) the entire ACRF. In this comparison we included counties with more than 80% agricultural land, corresponding to 70% of the counties. At the ACRF scale, predicted and 2002 Census mean vegetation cover matched well for all the cover types (Figure 4). Specifically, the low fractional cover of summer C_4 crop, intermediate fractions of summer and winter C_3 vegetation and forest, and large fraction of pastures were accurately predicted.

Large-scale spatial patterns in the county-aggregated predictions of 2002 land cover inferred using MODIS NDVI accurately matched those from the 2002 Census data (Figure 5). In both, there was a substantial difference in fractional coverage between the SE and the other three quadrants. Winter C_3 crop coverage is about 20% in the NW, NE, and SW quadrants, and about 55% in the SE quadrant. In contrast, pasture coverage is about 50-60% in the W, NE, and SW quadrants and about 30% in the SE quadrant.

We note two caveats relevant to this comparison. First, the 2002 Census data only included agricultural land, so a comparison of percent cover of each vegetation type was reasonable only if most of the land in a particular county was agricultural. Second, the comparison is only applicable in 2002, since there was substantial inter-annual variability in the types of crops planted, although the broad spatial patterns of vegetation cover were relatively stable. For example, 2003 had a relatively higher prevalence of winter C_3 crops and relatively lower prevalence of pasture. We discuss below the relationship between precipitation anomalies and fractional cover of the various crops.

Parameter Calibration

We calibrated V_m and C_s using the eddy covariance measurements; best-fit parameters are shown in Table 3 and simulations using these best-fit parameters are shown in Figure 6. These values are within the range of expected values for the various vegetation types [*Sellers, Randall et al.*, 1996]. We note that improvements to these parameter estimations could be made if more eddy covariance measurements were available. Overall, ISOLSM accurately simulated net ecosystem C exchange in these systems where observations were available for testing.

Soil Moisture

Soil moisture exerts a strong control on heterotrophic respiration, plant drought stress, surface evaporative fluxes, and other surface processes. On weekly to monthly time scales, inter-annual differences in near-surface (0-30 cm) soil moisture were temporally complex and not obviously related to annual precipitation. Soils in summer 2004 were consistently wetter than in summer 2003 in all vegetation cover types. However, soils were wetter in 2003 and 2005 (compared to 2004) in September in all vegetation cover types. There were no substantial early September rains in 2004, but there were October and November rains that caused soil moisture to be wetter than in either 2003 or 2005.

Regional NEE Estimates

We first present predictions from the 250 m simulations in the US Southern Great Plains, which were computed as vegetation-cover-weighted averages of ten 250 m cells per 10 km macro cell. We then compare these results to those obtained with simulations at coarser spatial scales and two scaling methods.

We calculated that the ACRF-SGP region was a net C sink, relative to the local atmospheric, for the three years simulated (Figure 7). Cumulative annual NEE was predicted to be -240, -340, and -270 g C m^{-2} y^{-1} for 2003, 2004, and 2005, respectively (implying an average annual net atmospheric C sink of about 2.8 t C ha^{-1}). Again, these estimates do not represent a 'true' sink, since some of the agricultural product is shipped out of the region, where it may be returned to the atmosphere relatively quickly.

Predicted spatial variability in midday NEE was large (e.g., Figure 8(a) shows midday NEE on April 15, 2003). At this time, C uptake was larger in the North-to-South band in the center of

the ACRF, consistent with Winter Wheat being near its peak LAI in this area. Further, cloud cover resulted in relatively larger solar radiation over the winter wheat belt, further enhancing the large-scale NEE spatial pattern.

Midday NEE spatial heterogeneity within each 10 km macrocell (indicated by the fractional-cover-weighted standard deviation of the 250 m simulations) was often as large as 75% of the mean and larger than the mean in about one-quarter of the macrocells (Figure 8(b)). This fine-scale variability resulted from large differences in LAI among the ten (for each vegetation cover type) 250 m gridcells in each 10 km macrocell. Spatial heterogeneity in nighttime NEE, which is comprised solely of ecosystem respiration, was much smaller than that of daytime NEE.

Inter-annual variability in regional-average NEE was substantial and resulted from several factors, including inter-annual variability in climate, fractional cover of vegetation types, and LAI for each cover type. For example, comparing 2003 and 2004, the difference in cumulative-annual NEE was partially caused by larger C uptake between March and May in 2004. This larger C uptake was driven by larger LAI in C_3 winter crop (~1 m^2 m^{-2} larger in 2004 than in 2003) and pasture (~0.5 m^2 m^{-2} larger) during this period. We note that 2004 was also the year with the highest cumulative precipitation, which may be responsible for the larger LAI. Also, air temperatures were higher during this period in 2003 than in 2004, leading to larger predicted soil respiration and therefore lower net ecosystem C uptake. Finally, there was also a large change in vegetation cover between 2003 and 2004 in which fractional cover of pasture increased from about 40 to 65% and C_3 winter crops decreased from about 31 to 20%.

Regional net C uptake was smaller in 2005 than 2004, with uptake by both C_3 winter crops and pasture contributing to this difference. The fractional cover of each vegetation type was relatively constant between 2004 and 2005. However, the LAI of C_3 winter crops was lower during the peak uptake period of March – May in 2005 than in 2004, as was LAI for pasture between April and June. Regional-mean pasture LAI in July and August 2005 was larger than it was in 2004; however, warmer temperatures during July and August in 2005 drove increased soil respiration C fluxes during this period.

Our calculations of NEE take into account the influence of a number of biophysical variables, such as cover type, LAI, precipitation, and temperature. We did not consider some other factors that can influence NEE, as described above, such as fertilizer type and application rate [*Fischer et al.*, 2007]. In addition, we did not predict land use or land cover, but rather

simulated NEE given land cover patterns. Predictions of future ecosystem fluxes in managed landscapes will have to use some method of predicting land cover and land management, which are functions of many factors, including farmers' decisions of what and when to plant and of economic forces (e.g., labor and fertilizer costs, crop subsidies). For example, recent demand and government incentives for biofuel crops (i.e., corn) are driving increases in corn production in many of the Great Plains states [*Barrionuevo*, 2006].

Regional Latent Heat Fluxes and Water Use Efficiency

Spatial heterogeneity in LH fluxes was smaller than it was in NEE, although broad spatial patterns in the two fluxes were consistent (compare Figure 8(a) and Figure 8(c), which show NEE and LH for noon on April 15, 2003). As described above for NEE, the pattern at this point in time is consistent with the active Winter Wheat and solar radiation distributions. Spatial heterogeneity in midday LH (calculated as for NEE above) was usually less than 10% of the mean in each 10 km macro-cell. Inter-annual differences in predicted weekly LH fluxes were smaller than for NEE. Variation in weekly LH fluxes was smallest in 2004, the year with the most precipitation.

Consistent with stomatal control of CO_2 assimilation and transpiration (e.g., [*Collatz et al.*, 1991]), daytime, weekly, regional latent-heat flux (L) predicted at the 250 m scale was correlated with GPP (Figure 9; $R^2 = 0.72$; note that only weeks with $L > 50$ W m^{-2} are included). The slope of the line for predicted cumulative GPP versus cumulative L, a measure of water use efficiency (WUE, g C kg^{-1} H_2O), was relatively consistent among years; the average annual WUE for all three years for the region was 3.4 g C kg^{-1} H_2O. This value is consistent with those found by Law et al. [2002] in their analysis of FLUXNET data, who reported slopes of 3.4, 3.2, and 3.1 g C kg^{-1} H_2O for grasslands, deciduous broadleaf forests, and crops, respectively. Law et al. [2002] also tested whether a vapor pressure deficit weighted WUE (WUE-VPD; calculated as g C assimilated per kg H_2O lost multiplied by vapor pressure deficit) correlated with GPP, and found poorer correlation, although this metric has been applied to estimate large-scale C exchanges [*Beer et al.*, 2007]. Consistent with the FLUXNET analysis [*Law et al.*, 2002], we found a poorer correlation ($R^2 = 0.5$) between WUE-VPD and GPP.

Effect of Spatial Resolution on Regional Predictions

To determine how the spatial resolution of simulations affected predictions of surface fluxes in a region with fine-scale spatial heterogeneity, we performed two series of model runs at 10, 30, 60, and 90 km resolutions. First, we applied a single dominant vegetation cover type and average LAI in each grid cell to calculate the NEE and LH values for each cell. Second, we applied the mean LAI of each cover type in each grid cell to estimate each cover type's surface exchanges, and then weighted these estimates by the fractional cover within the cell to calculate NEE and LH for each grid cell. The resulting regional fluxes were then compared to predictions at 250 m resolution.

Predicted annual cumulative regional NEE in 2003 using the dominant cover approach was -280, -370, -400, and -340 g C m^{-2} y^{-1} at 10, 30, 60, and 90 km, respectively, and in 2004 was -390, -410, -410, and -410 g C m^{-2} y^{-1} for the same set of spatial resolutions (Figure 10(a, c)). Maximum biases compared to the cumulative annual regional NEE calculated at the 250 m scale were 70% and 20% in 2003 and 2004, respectively. Biases of over 100% occurred in both years for weekly integrated NEE; the fractional bias was largest in winter when NEE is typically small. In both years, the regional average assimilation was higher when predicted at the coarser scales than at the 250 m scale. This bias resulted from a combination of the increasing dominance of pasture over C_3 winter crop as scale increased and the larger C assimilation by pasture. The effect was stronger in 2004 because more than 90% of the surface was characterized as pasture at the 90 km scale.

The second approach (which is used in many current land-surface models) led to regional annual estimates of up to 25% more net C uptake than the 250 m simulations in 2003 (Figure 10(b)) and 2004 (Figure 10(d)). Weekly biases, between 10 and 50% during the growing season, were also smaller than for the dominant cover scaling. At all scales, weekly biases in predicted assimilation and ecosystem respiration were smaller (~10%) than for NEE, but when combined to predict NEE led to larger fractional biases than for either flux alone.

Simulations at coarser resolutions consistently predicted more C uptake than those at the 250 m scale. This bias resulted primarily from using the mean of the 250 m LAI values, even though the LAI had a distribution that was consistently more lognormal than symmetric, for each cover type across the larger grid cell (Figure 11). We note also that, even for a symmetric LAI distribution, a single NEE calculated using the mean LAI may differ from a mean NEE

calculated across the LAI distribution. Such a discrepancy can occur because canopy assimilation is, in general, non-linearly related to LAI due to the changing proportion of leaves in shaded and sunlit conditions, leaf clumping, and other factors [*Chen et al.*, 2008]. Thus, achieving accurate NEE estimates with simulation resolutions that are much coarser than the spatial heterogeneity in cover type and LAI requires a more sophisticated sampling approach than simply using the mean LAI for each cover type in the grid cell. An example approach would be to characterize the LAI probability density function (pdf) of each grid cell by a geometric mean and geometric standard deviation, and then evenly distribute a subset of 250 m grid cell simulations across the LAI range. The grid cell NEE for each cover type would be calculated using the pdf to weight the predictions across the grid cell. Finally, the overall NEE across the grid cell would be calculated by weighting the NEE from each cover type by its fractional cover within the grid cell.

The effect of spatial resolution on regional weekly average LH fluxes was smaller than it was for NEE (Figure 12), but somewhat larger than for either assimilation or respiration. The largest summer and winter biases were ~30 and 20%, respectively. Similar to NEE, the second approach to scaling LH (i.e., weighting by fractional cover predictions in each gridcell that used the mean LAI of each cover type) had lower biases than using the dominant vegetation cover (not shown).

There were substantial spatial gradients in weekly LH fluxes across the ACRF that were missed by the coarse-scale simulation. During midday, for example, LH spatial gradients across the region of hundreds of W m^{-2} are common (Figure 8(c)). Similarly, temporal averaging obscured important diurnal variations. These variations are caused by both slowly (e.g., LAI) and rapidly (e.g., clouds) varying system characteristics. Therefore, for applications that require accurate characterization of the surface energy budget at diurnal or sub-diurnal time scales or 10-100 km spatial scales (e.g., cloud models), including details of variability in climate forcing, cover type, and LAI is required.

A number of studies have examined the impacts of spatial heterogeneity on predicted surface fluxes in non-agricultural systems. Li et al. [2008] studied the effect of spatial heterogeneity on surface LH and SH fluxes in southern Arizona using Landsat images and a model based on measured radiometric surface temperature and vegetation cover fraction. They concluded that LH and SH were well estimated using 30 m and 120 m estimates (which were at

or below the scale of local vegetation heterogeneity), but the accuracy deteriorated for lower resolution, particularly for LH fluxes. Kimball et al. [1999] studied spatial scaling issues (with land-cover characteristics specified from 30 m to 50 km) within the boreal forest of the BOREAS project [*Sellers et al.*, 1997]. Compared to the high-resolution results, they concluded that predictions at the coarser scales resulted in large monthly NPP biases (28 to 48%), but that annual NPP biases were lower (2 to 14%), primarily because of offsetting errors. They also reported lower monthly LH bias (<5%) as compared to NPP biases, again due to partial compensation of model errors. Our results showed similar patterns: i.e., predicted annual NEE biases were smaller than many of the weekly average biases, and predicted weekly biases in LH were smaller than for NEE.

Chen et al. [2007] showed, with a land-surface model applied across Canada, that differences of up to 25% in surface fluxes were predicted with a dominant cover and a fractionally distributed vegetation cover, indicating that different methods of treating subgrid heterogeneities could lead to biases in surface fluxes. For comparison, our simulations had annual cumulative NEE differences between the dominant and fractionally distributed cases as large as 40%, with an average difference of 10%. Turner et al. [2000], in a Pacific Northwest forest, used Landsat 25 m data to study land cover classification and predicted C exchanges across scales up to 1 km. At resolutions coarser than 250 m the pattern of clear-cuts was lost and the land-cover classification agreement at the coarsest scale was relatively pool. Predicted NPP and tree biomass decreased and increased, respectively, with increasing scale. Our estimates of bias associated with the spatial resolution at which agricultural land cover type and status are specified are comparable to those found in these forest studies, as is our observation that LH estimates were somewhat less sensitive to resolution than NEE estimates.

We also note that biases in predicted surface fluxes depend on the extent to which the flux of interest depends on land-cover type and its status. Other trace gases of agricultural interest, such as N_2O and CH_4, also depend strongly on these system properties, and therefore we also expect them to vary strongly across spatial scales of system characterization.

As mentioned above, inverse methods are being used to estimate regional C and energy exchanges. The first phase of the ongoing NACP Mid-Continent Intensive (MCI) study (http://nacp.ornl.gov/mast-dc/int_synth_mci.shtml) ('interim synthesis') includes compilation and comparison of top-down and bottom-up estimates for a region in the Central U.S. For

comparison to our results, we extracted results at 1×1° resolution from three inversion models (CarbonTracker [*Peters et al.*, 2007], UT [*Deng et al.*, 2007], and LSCE [*Chevallier et al.*, 2005], CSU [Schuh et al., 2009] that spanned at least one year of the three-year period of our study. We note that other groups are preparing results for the interim synthesis, but those results were unavailable at the time this paper was finalized. For comparison to the bottom-up predictions, we averaged the inversions predictions to a 3°×3° region centered on the ACRF (Figure 13). The inversions are global in scale, with different spatial resolutions, constraining observations, inversion approaches, and downscaling methods; these differences are reflected in the relatively large range of NEE estimates.

Given uncertainties in both the inversion and our bottom-up estimates, it is currently impossible to rank one NEE estimate as superior to the other. However, comparisons between the approaches can highlight periods, system properties, or regions for further study and model improvement. For this study, we note that the late spring peak NEE drawdowns were comparable between the bottom-up and LSCE inversion predictions, and that net C release during the winter was comparable between the bottom-up and CarbonTracker predictions. For 2004, the CSU model and bottom-up approach predicted similar seasonal cycles, but somewhat different peak values in summer. Both the UT and LSCE inversions predicted a large net ecosystem C efflux during summer, which was not predicted in either the CarbonTracker or our bottom-up approach. Further analyses could focus on these differences to improve both the bottom-up and top-down regional C exchange estimates of the region.

Conclusions

We presented bottom-up C and latent heat exchange predictions in a spatially heterogeneous agricultural region in the Southern Great Plains (ACRF-SGP). The region was predicted to be a net C sink, with respect to the local atmosphere, of -240, -340, and -270 g C m^{-2} y^{-1} for 2003, 2004, and 2005, respectively. We note that, in contrast to many forested systems, much of the accumulated biomass represented in this sink may be transported horizontally where it can be rapidly returned to the atmosphere. Both NEE and latent heat fluxes were spatially and temporally heterogeneous, arguing that accurate representation of surface exchanges in this system must account for observed heterogeneity in cover type and vegetation status.

Conducting simulations at coarser resolution led to biases in the predicted net ecosystem fluxes, with the magnitude of bias depending on the scaling approach. We predicted differences up to 25% in annual C exchange estimates between the 250 m approach and those based on fractional cover and means of LAI (in 10, 30, 60, and 90 km gridcells) for each cover type. This scaling approach, used in current land-surface models, resulted in errors this large (and larger for weekly averages) because of the heterogeneous LAI distribution within land cover types. However, even a symmetric LAI distribution does not guarantee that a single NEE calculated using the mean LAI will be the same as the cumulative NEE calculated across the LAI distribution. Predicted latent heat flux biases across scales were smaller than those for C exchanges, but somewhat larger than biases for gross primary production and ecosystem respiration. Not surprisingly, using a single dominant vegetation cover for each gridcell resulted in even larger biases in surface exchanges. Coarse spatial and temporal resolution simulations also obscured important variations across the region.

Our results suggest several steps to improve regional-scale, bottom-up, ecosystem C exchange predictions. First, although using observed LAI had the advantage of capturing year-to-year variation in cover type and management effects, variations in fertilizer application rate and type, irrigation practices, and planting methods also affect C exchanges [*Fischer et al.*, 2007] and need to be included in a robust modeling framework. Using observed LAI also precludes predictions of future system behavior. Second, our approach to characterizing vegetation type could be improved with more observations of cover type and LAI in the region. These measurements need to be made at the scale at which cover type varies, i.e., on the order of a hundred meters. Finally, independent methods of estimating regional-scale fluxes need to be made and compared with bottom-up estimates. For example, the top-down approaches described above, as well as boundary layer budgeting approaches [*Bakwin et al.*, 2004; *Helliker et al.*, 2004; *Lai et al.*, 2006; *Wang et al.*, 2007; *Williams et al.*, 2005], show promise in this regard. A combination of approaches will likely be required to establish confidence in regional NEE estimates in heterogeneous landscapes such as the one studied here.

Acknowledgments

This work was supported by the Director, Office of Science, Office of Biological and Environmental Research, Climate Change Research Division, of the U.S. Department of Energy under Contract No. DE-AC02-05CH11231. This study was also part of the North American

Carbon Program. The MTI image was provided by the Office of Nonproliferation and National Security of the U.S. Department of Energy. We also thank the groups making their MCI inversion results available: CarbonTracker 2008 results provided by NOAA ESRL, Boulder, Colorado, USA from the website at http://carbontracker.noaa.gov; UT results provided by Jing Chen, University of Toronto, Canada; and LSCE results provided by Frederic Chevallier, Laboratoire des Sciences du Climat et de l'Environnement, France.

Tables

LSM1 Surface Cover Type	*USDA Agriculture Census Cover Types for ACRF-SGP*
Summer C_3 crop	Sunflower, cotton, soy, dry beans, forage, peanuts, orchard, vegetables, potatoes, beets, irrigated crop, other crop
Winter C_3 crop	Winter wheat, barley, oat, rye, grazed crop
Summer C_4 crop	Corn, sorghum
Pasture	Range
Forest	Wood

Table 1. Mapping of cover types contained in the USDA Agricultural Census of Oklahoma and Kansas to the seven cover types simulated in ISOLSM.

Surface Cover Type	*2002*	*2003*	*2004*
Wheat	Jan – Jun	Jan – Dec	Jan – Dec
	Apr – Jun	Apr – June	Apr – Jun
	Apr – Jun		
Pasture	Jun – Aug	Apr – Aug	Apr – Nov
	Jun – Aug		
Sorghum		Jun – Aug	Jun – Nov

Table 2. Data available from the eddy correlation towers for parameter determination (2002, 2003) and testing (2004) of the calibrated model.

Parameter	*Winter C_3 Crop (Wheat)*	*Pasture C_3 Grass*	*Pasture C_4 Grass*	*Summer C_4 Crop (Sorghum)*

S_c (kg C m^{-2})	20	14	14	12
V_m (μmol m^{-2} s^{-1})	99	70	20	21

Table 3. Best-fit parameters used in the simulations.

Extended Facility Name	**Specific Humidity (g g^{-1})**			**Pressure (kPa)**			**Temperature (ºC)**		
	Error	*RMSE*	*R*	*Error*	*RMSE*	*R*	*Error*	*RMSE*	*R*
E13	*-1.0e-4*	*1.2e-5*	*0.94*	*-0.01*	*3.9e-4*	*1.00*	*0.24*	*7.0e-3*	*1.00*
E15	*1.3e-4*	*5.8e-6*	*0.99*	*-0.27*	*3.5e-4*	*1.00*	*0.02*	*7.9e-3*	*1.00*
E21	*-2.7e-4*	*5.4e-6*	*0.99*	*-0.11*	*3.3e-4*	*1.00*	*0.24*	*1.0e-2*	*0.99*
E24	*5.9e-5*	*4.0e-6*	*0.99*	*0.22*	*3.4e-4*	*1.00*	*0.01*	*6.5e-3*	*1.00*

Table 4. Comparison between interpolated and measured atmospheric specific humidity, pressure, and temperature at four Oklahoma ARM extended facilities sites not used in the interpolation. Extended Facilities locations used in the comparison: E13 (97.485W, 36.605N); E15 (98.284W, 36.431N); E21 (96.065W, 35.615N); E24 (98.205W, 34.883N).

Figures

Figure 1. July 2001 Los Alamos National Laboratory multispectral thermal imager view of the fields surrounding the ACRF-SGP Central Facility. The mosaic of harvested crops, growing crops, and pasture emphasizes the heterogeneity of land-cover in the Southern Great Plains.

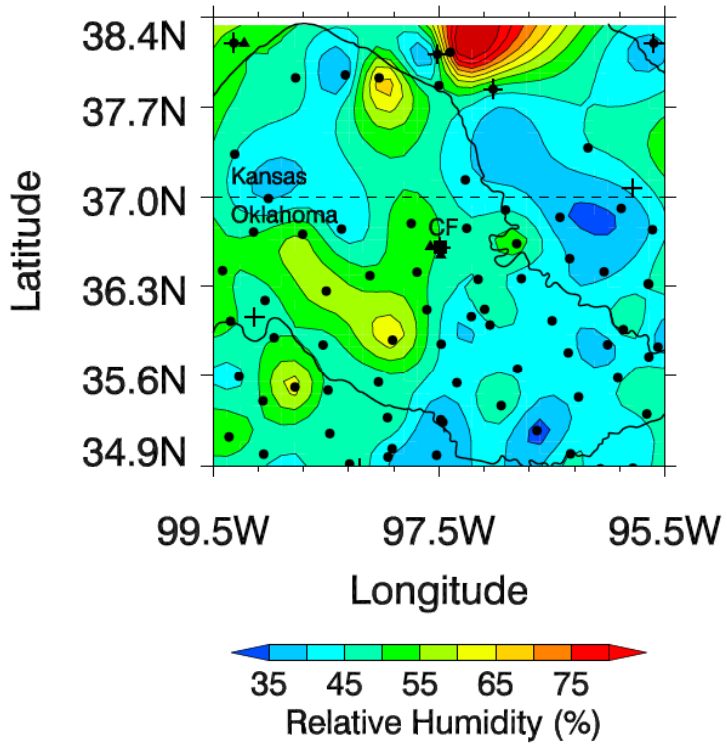

Figure 2. Oklahoma and Kansas Mesonet platforms (solid circles), portable eddy covariance sites (triangles), Extended Facility eddy covariance towers (+), and Central Facility 60 m tower (square). The contours show surface relative humidity over the ARM-SGP domain on March 22 2003 at 00:00.

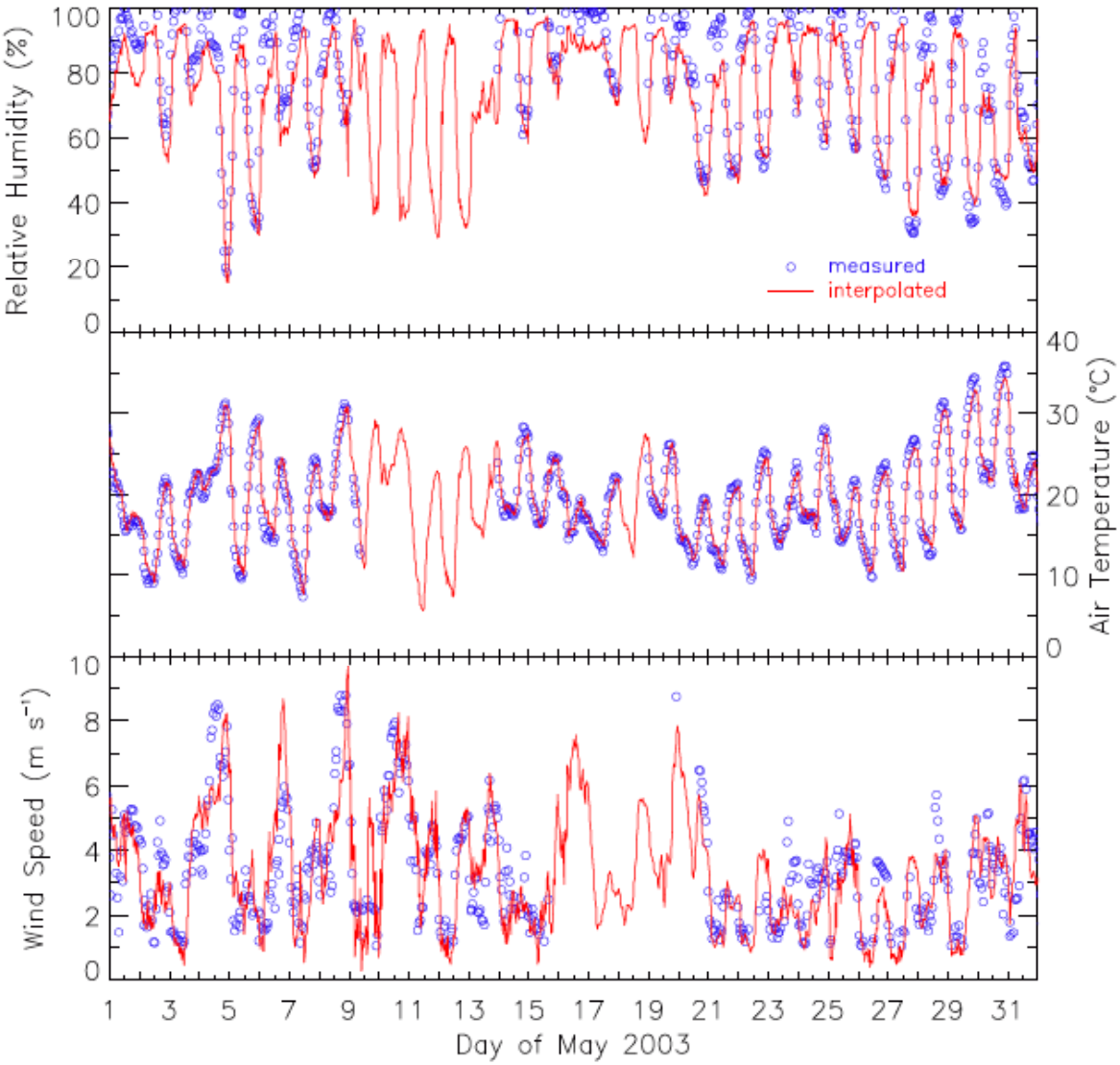

Figure 3. Example of interpolated and measured (a) air temperature, (b) wind speed, and (c) relative humidity at the Central Facility wheat site.

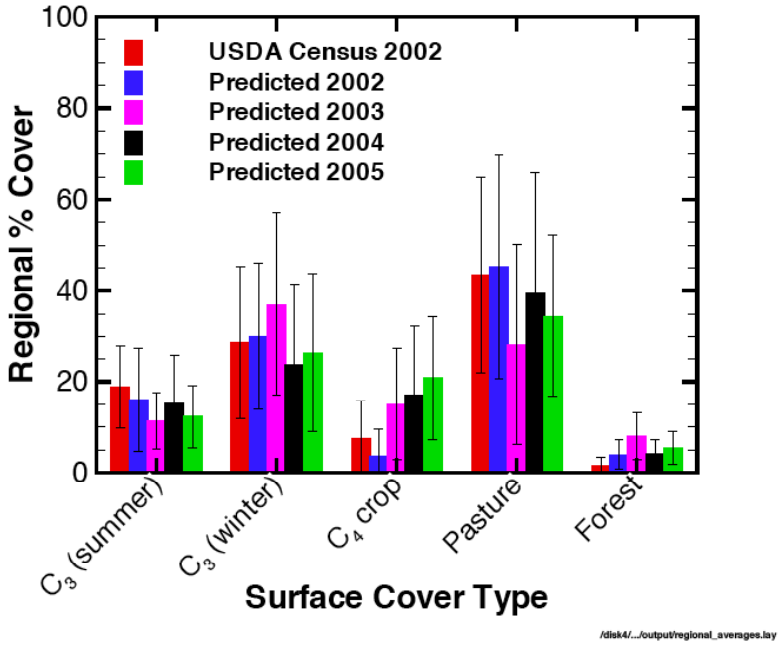

Figure 4. ACRF regional average (error bars show SD) percent vegetation cover determined from the MODIS NDVI and 2002 Census data. Counties with more than 80% land area covered by agriculture are included. The vegetation type characterization using the 2002 MODIS NDVI data closely matched the results of the 2002 USDA Census.

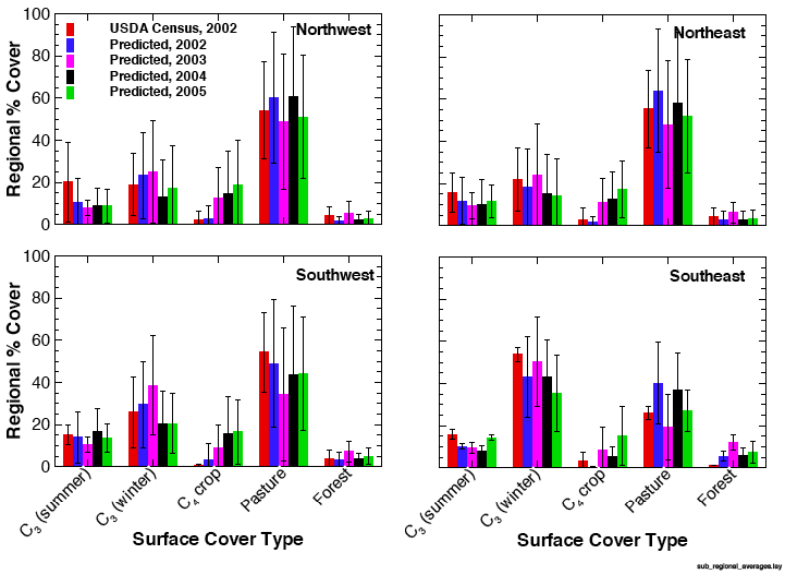

Figure 5. Average (error bars show SD) percent vegetation cover for four quadrants (NW, NE, SW, and SE) in the ACRF determined from the MODIS NDVI and the 2002 USDA Census. Counties with more than 80% land area covered by agriculture are included. The vegetation type characterization using MODIS NDVI data closely matched the results from the 2002 USDA

Census, and captured the large-scale spatial variability in C_3 winter crop versus pasture fractional cover.

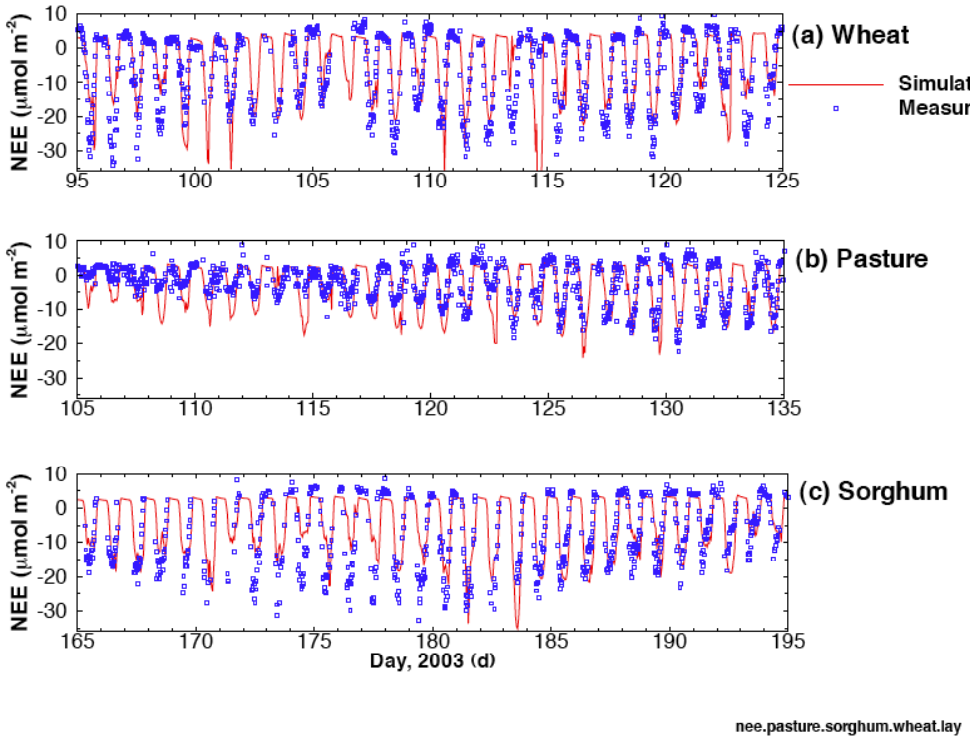

Figure 6. NEE estimates from portable eddy covariance measurements and ISOLSM used for model calibrations for (a) wheat, (b) pasture, and (c) sorghum. The corresponding best-fit parameters are given in Table 3.

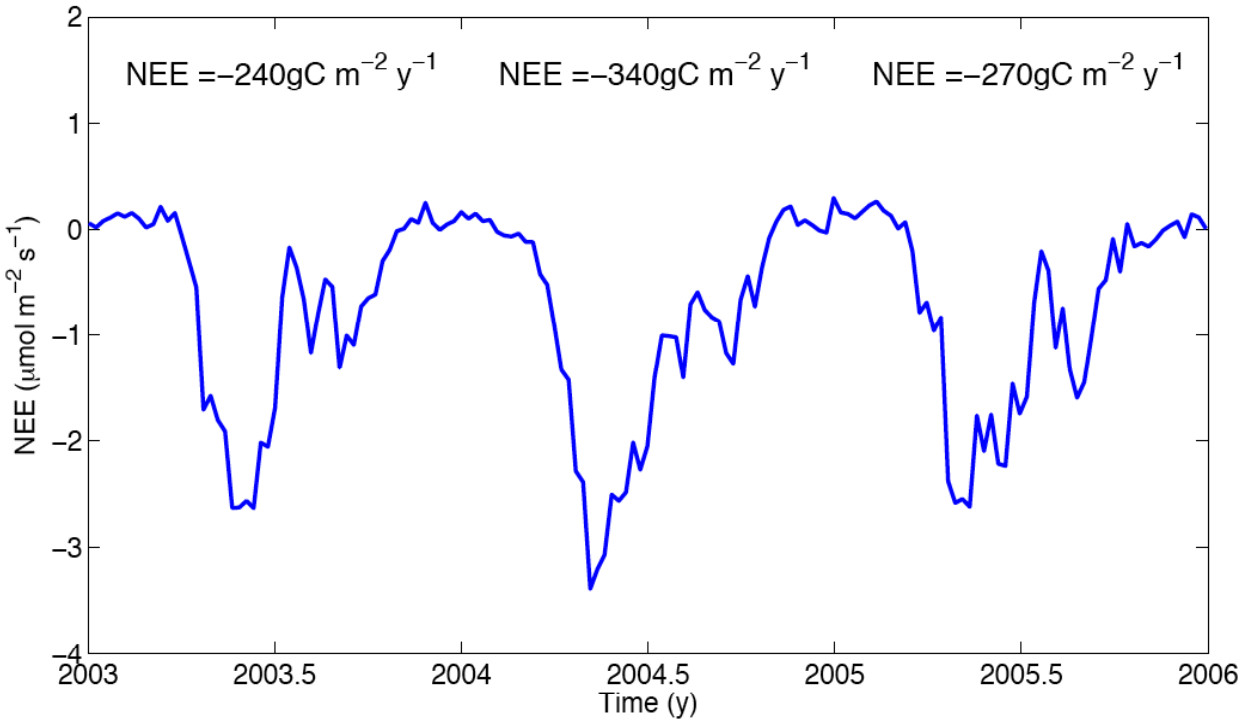

Figure 7. Predicted NEE for the ACRF region. Annual cumulative NEE is shown for each of the three years. Regional NEE seasonality and inter-annual variability depends strongly on vegetation cover type fractional cover and status.

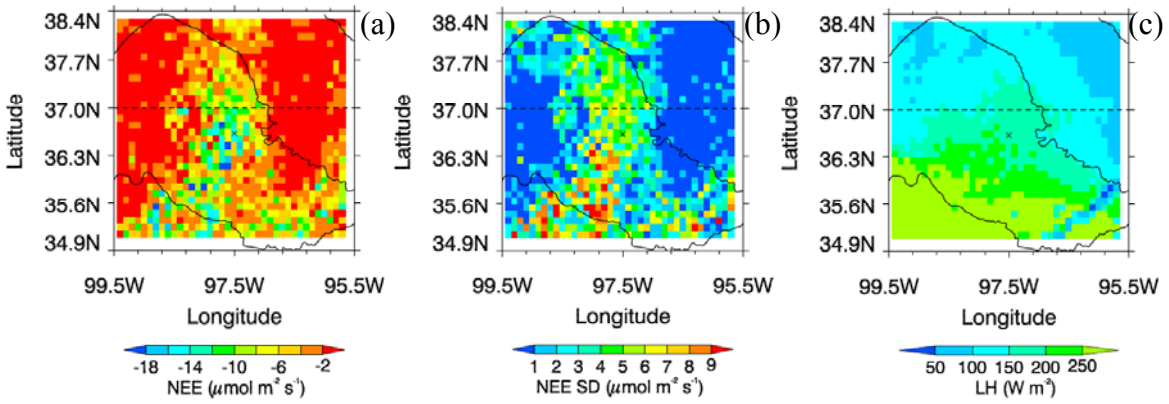

Figure 8. For noon, April 15, 2003: (a) NEE (b) Fractional-cover-weighted standard deviation of NEE; and (c) LH flux. NEE spatial variation (SD) within the 10 km gridcells at a particular time can be larger than the mean in the gridcell, while LH fluxes are typically much less heterogeneous than NEE.

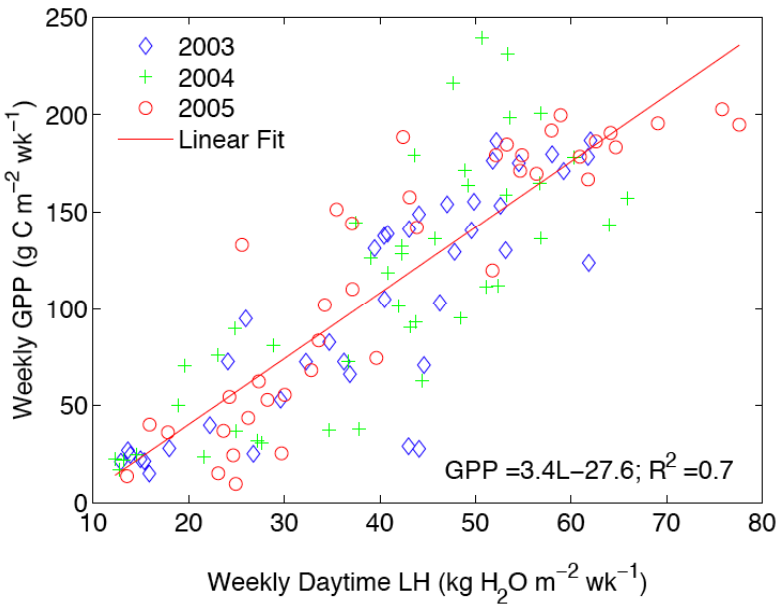

Figure 9. Weekly regional cumulative GPP versus weekly regional cumulative daytime latent heat flux (for weeks with L > 50 W m^{-2}).

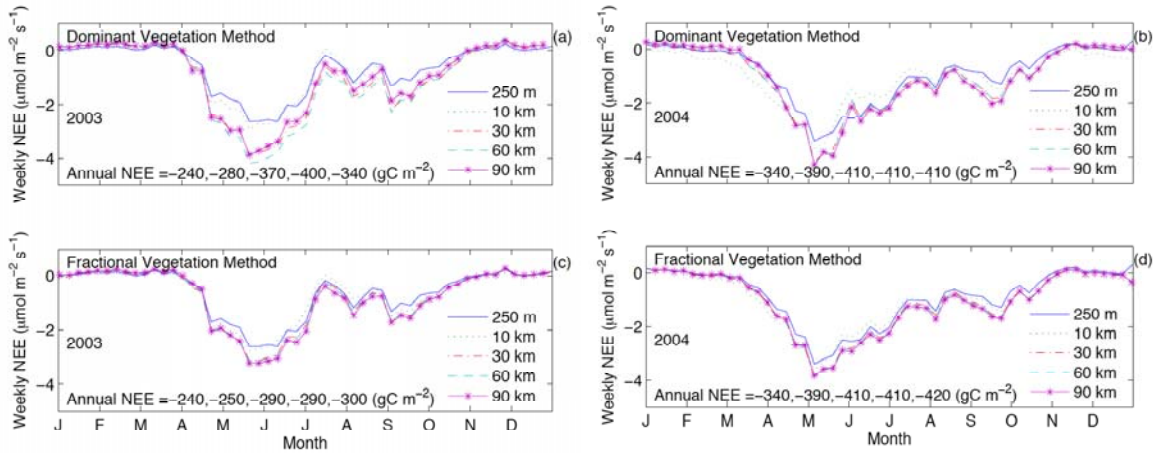

Figure 10. Weekly ACRF-SGP NEE estimates for two scaling methods and five spatial scales: 250 m, 10 km, 30 km, 60 km, and 90 km for 2003 (a, c) and 2004 (b, d). For both methods, the region was predicted to become a stronger C sink at the larger resolutions than at the 250 m resolution. For the 'fractional vegetation method', annual NEE differed by ~5 and 20% between the 250 m and larger scale estimates in 2003 and 2004, respectively.

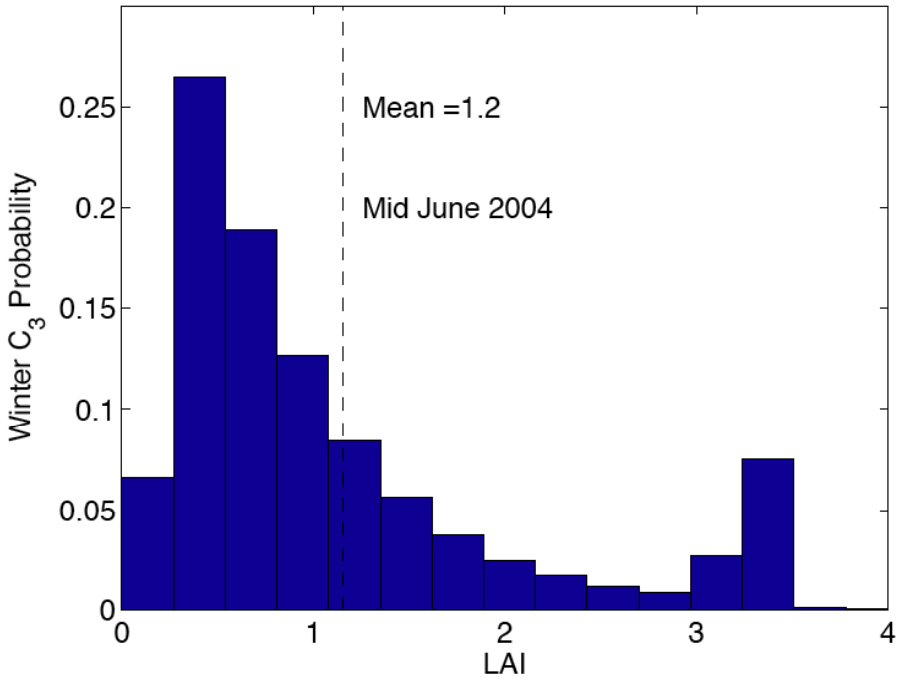

Figure 11. LAI probability density for winter wheat in the 250 m gridcells across the ACRF domain in mid-June, 2004. This distribution is common in the ACRF, and demonstrates one reason why the mean LAI does not accurately represent the vegetation when estimating NEE.

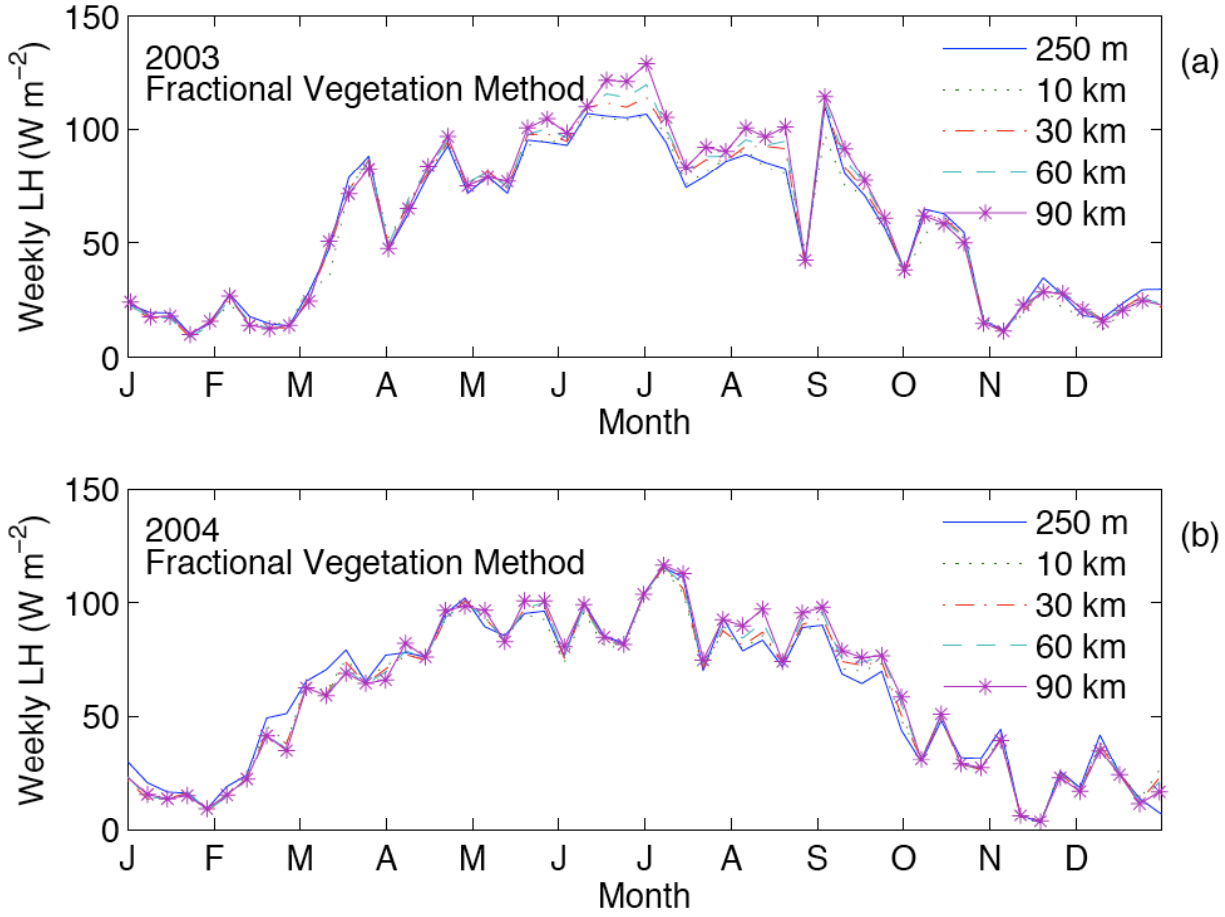

Figure 12. Weekly LH flux estimates, using the dominant vegetation cover type in each cell, for five spatial scales: 250 m, 10 km, 30 km, 60 km, and 90 km for (a) 2003 and (b) 2004. Differences between scales were much smaller than those for NEE (Figure 10(a, b)).

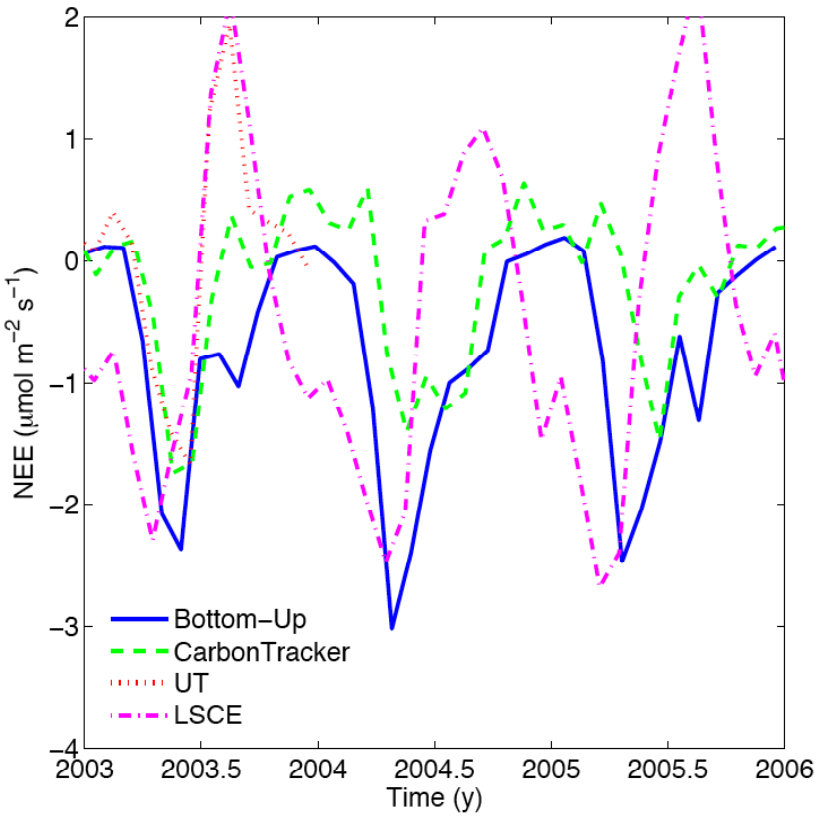

Figure 13. Comparison between the bottom-up regional NEE predictions and four top-down inversion predictions (averaged over a 3°×3° region centered over the ACRF) prepared for the NACP MCI study.

References

Ackerman, T. P., A. D. D. Genio, R. G. Ellingson, R. A. Ferrare, S. A. Klein, G. M. McFarquhar, P. J. Lamb, C. N. Long, and J. Verlinde (2004), Atmospheric Radiation Measurement Program Science Plan: Current Status and Future Direcitons of the ARM Science Program, U. S. Department of Energy, Office of Biological and Environmental Research.

Aranibar, J. N., J. A. Berry, W. J. Riley, D. E. Pataki, B. E. Law, and J. R. Ehleringer (2006), Combining meteorology, eddy fluxes, isotope measurements, and modeling to understand environmental controls of carbon isotope discrimination at the canopy scale, *Global Change Biology*, *12*,ISI:000236549600010, 710-730.

Bachelet, D., R. Neilson, J. Lenihan, and R. Drapek (2001), Climate change effects on vegetation distribution and carbon budget in the United States *Ecosystems*, *4*164-185.

Bakwin, P., K. Davis, C. Yi, S. Wofsy, J. Munger, L. Haszpra, and Z. Barcza (2004), Regional carbon dioxide fluxes from mixing ratio data, *Tellus Series B-Chemical AND Physical Meteorology*, *56*301-311.

Barrionuevo, A. (2006), Crop rotation in the Grain Belt, in *New York Times*, edited, New York, NY.

Beer, C., M. Reichstein, P. Ciais, G. D. Farquhar, and D. Papale (2007), Mean annual GPP of Europe derived from its water balance, *Geophysical Research Letters*, *34*,WOS:000244897200007.

Billesbach, D. P., M. L. Fischer, M. S. Torn, and J. A. Berry (2004), A portable eddy covariance system for the measurement of ecosystem-atmosphere exchange of CO2, water vapor, and energy, *Journal of Atmospheric and Oceanic Technology*, *21*,ISI:000220648500009, 639-650.

Bonan, G. B., F. S. Chapin, III, and S. L. Thompson (1995), Boreal forest and tundra ecosystems as components of the climate system, *Climatic Change*, *29*145-168.

Bonan, G. B. (1996), A land surface model (LSM version 1.0) for ecological, hydrological, and atmospheric studies: Technical description and user's guide, 150 pp, NCAR, Boulder, CO.

Bonan, G. B., K. J. Davis, D. Baldocchi, D. Fitzgerald, and H. Neumann (1997), Comparison of the NCAR LSM I land surface model with BOREAS aspen and jack pine tower fluxes, *Journal of Geophysical Research*, *102*29,065-029,076.

Bonan, G. B., K. W. Oleson, M. Vertenstein, S. Levis, X. B. Zeng, Y. J. Dai, R. E. Dickinson, and Z. L. Yang (2002), The land surface climatology of the community land model coupled to the NCAR community climate model, *Journal of Climate*, *15*,609CJ-0002 609CJ: Document Delivery available, 3123-3149.

Brock, F. V., K. C. Crawford, R. L. Elliott, G. W. Cuperus, S. J. Stadler, H. L. Johnson, and M. D. Eilts (1995), The Oklahoma Mesonet - a Technical Overview, *Journal of Atmospheric and Oceanic Technology*, *12*,ISI:A1995RD05800002, 5-19.

Chen, B. Z., J. M. Chen, G. Mo, C. W. Yuen, H. Margolis, K. Higuchi, and D. Chan (2007), Modeling and scaling coupled energy, water, and carbon fluxes based on remote sensing: An application to Canada's landmass, *Journal of Hydrometeorology*, *8*,ISI:000246061100002, 123-143.

Chen, Q., D. Baldocchi, P. Gong, and T. Dawson (2008), Modeling radiation and photosynthesis of a heterogeneous savanna woodland landscape with a hierarchy of model complexities, *Agricultural and Forest Meteorology*, *148*,ISI:000257006200015, 1005-1020.

Chevallier, F., M. Fisher, P. Peylin, S. Serrar, P. Bousquet, F. M. Breon, A. Chedin, and P. Ciais (2005), Inferring CO2 sources and sinks from satellite observations: Method and application to TOVS data, *Journal of Geophysical Research-Atmospheres*, *110*,ISI:000234506500004.

Collatz, G. J., J. T. Ball, C. Grivet, and J. A. Berry (1991), Physiological and environmental regulation of stomatal conductance, photosynthesis and transpiration: a model that includes a laminar boundary layer, *Agricultural and Forest Meteorology*, *54*107-136.

Collins, W., C. Bitz, M. Blackmon, G. Bonan, C. Bretherton, J. Carton, P. Chang, S. Doney, J. Hack, T. Henderson, J. Kiehl, W. Large, D. McKenna, B. Santer, and R. Smith (2006), The Community Climate System Model version 3 (CCSM3), *Journal of Climate*, *19*2122-2143.

Coops, N. C., T. A. Black, R. P. S. Jassal, J. A. T. Trofymow, and K. Morgenstern (2007), Comparison of MODIS, eddy covariance determined and physiologically modelled gross primary production (GPP) in a Douglas-fir forest stand, *Remote Sensing of Environment*, *107*,ISI:000245827500001, 385-401.

Dai, Y. J., X. B. Zeng, R. E. Dickinson, I. Baker, G. B. Bonan, M. G. Bosilovich, A. S. Denning, P. A. Dirmeyer, P. R. Houser, G. Y. Niu, K. W. Oleson, C. A. Schlosser, and Z. L. Yang (2003), The Common Land Model, *Bulletin of the American Meteorological Society*, *84*,ISI:000184829200015, 1013-+.

Deng, F., J. M. Chen, M. Ishizawa, C. W. Yuen, G. Mo, K. Higuchi, D. Chan, and S. Maksyutov (2007), Global monthly CO2 flux inversion with a focus over North America, *Tellus Series B-Chemical and Physical Meteorology*, *59*,ISI:000245628900003, 179-190.

Desai, A. R., A. Noormets, P. V. Bolstad, J. Q. Chen, B. D. Cook, K. J. Davis, E. S. Euskirchen, C. M. Gough, J. G. Martin, D. M. Ricciuto, H. P. Schmid, J. W. Tang, and W. G. Wang (2008), Influence of vegetation and seasonal forcing on carbon dioxide fluxes across the Upper Midwest, USA: Implications for regional scaling, *Agricultural and Forest Meteorology*, *148*,ISI:000254022900011, 288-308.

Dickinson, R. E., A. Henderson-Sellers, P. J. Kennedy, and M. F. Wilson (1986), *Biosphere/atmosphere transfer scheme (BATS) for the NCAR community climate model. NCAR Technical Note TN275*, National Center For Atmospheric Research, Boulder, Colorado.

Doran, J. C., J. M. Hubbe, J. C. Lijegren, W. J. Shaw, G. J. Collatz, D. R. Cook, and R. L. Hart (1998), A technique for determining the spatial and temporal distribution of surface fluxes of heat and moisture over the Southern Great Plains Cloud and Radiation Testbed, *Journal of Geophysical Research*, *103*6109-6121.

Field, C. B., M. J. Behrenfeld, J. T. Randerson, and P. Falkowski (1998), Primary production of the biosphere: integrating terrestrial and oceanic components, *Science*, *281*237-240.

Fischer, M. L., D. P. Billesbach, W. J. Riley, J. A. Berry, and M.S.Torn (2007), Spatiotemporal Variations in Growing Season Exchanges of CO_2, H_2O, and Sensible Heat in Agricultural Fields of the Southern Great Plains, *Earth Interactions*, *11*1-21.

Fulton, R. A., J. P. Breidenbach, D. J. Seo, D. A. Miller, and T. O'Bannon (1998), The WSR-88D rainfall algorithm, *Weather and Forecasting*, *13*,ISI:000075402600013, 377-395.

Gerbig, C., J. C. Lin, S. C. Wofsy, B. C. Daube, A. E. Andrews, B. B. Stephens, P. S. Bakwin, and C. A. Grainger (2003), Toward constraining regional-scale fluxes of CO2 with atmospheric observations over a continent: 2. Analysis of COBRA data using a receptor-oriented framework - art. no. 4757, *Journal of Geophysical Research-Atmospheres*, *108*,760WM-0010 760WM: Document Delivery available, 4757.

Goetz, S. J., S. D. Prince, S. N. Goward, M. M. Thawley, and J. Small (1999), Satellite remote sensing of primary production: an improved production efficiency modeling approach, *Ecological Modelling*, *122*,ISI:000083474100008, 239-255.

Gu, L. H., D. Baldocchi, S. B. Verma, T. A. Black, T. Vesala, E. M. Falge, and P. R. Dowty (2002), Advantages of diffuse radiation for terrestrial ecosystem productivity - art. no. 4050 [Review], *Journal of Geophysical Research-Atmospheres*, *107*,609FJ-0009 609FJ: Document Delivery available, 4050.

Gurney, K. R., R. M. Law, A. S. Denning, P. J. Rayner, D. Baker, P. Bousquet, L. Bruhwiler, Y. H. Chen, P. Ciais, S. M. Fan, I. Y. Fung, M. Gloor, M. Heimann, K. Higuchi, J. John, E. Kowalczyk, T. Maki, S. Maksyutov, P. Peylin, M. Prather, B. C. Pak, J. Sarmiento, S. Taguchi, T. Takahashi, and C. W. Yuen (2003), TransCom 3 CO_2 inversion intercomparison: 1. Annual mean control results and sensitivity to transport and prior flux information, *Tellus Series B-Chemical and Physical Meteorology*, *55*,ISI:000182698400042, 555-579.

Heinsch, F. A., M. S. Zhao, S. W. Running, J. S. Kimball, R. R. Nemani, K. J. Davis, P. V. Bolstad, B. D. Cook, A. R. Desai, D. M. Ricciuto, B. E. Law, W. C. Oechel, H. Kwon, H. Y. Luo, S. C. Wofsy, A. L. Dunn, J. W. Munger, D. D. Baldocchi, L. K. Xu, D. Y. Hollinger, A. D. Richardson, P. C. Stoy, M. B. S. Siqueira, R. K. Monson, S. P. Burns, and L. B. Flanagan (2006), Evaluation of remote sensing based terrestrial productivity from MODIS using

regional tower eddy flux network observations, *Ieee Transactions on Geoscience and Remote Sensing*, *44*,ISI:000238864700022, 1908-1925.

Helliker, B. R., J. A. Berry, A. K. Betts, P. S. Bakwin, K. J. Davis, A. S. Denning, J. R. Ehleringer, J. B. Miller, M. P. Butler, and D. M. Ricciuto (2004), Estimates of net CO_2 flux by application of equilibrium boundary layer concepts to CO_2 and water vapor measurements from a tall tower, *Journal of Geophysical Research-Atmospheres*, *109*,ISI:000224876600002.

IPCC (2007), *Climate Change 2007: The Physical Science Basis. Contribution of Working Group I to the Fourth Assessment Report of the IPCC*, Cambridge University Press, Cambridge, United Kingdom and New York.

Jarvis, P. G. (1995), Scaling processes and problems, *Plant, Cell and Enviroment*, *18*1079-1090.

Jones, J. W., G. Hoogenboom, C. H. Porter, K. J. Boote, W. D. Batchelor, L. A. Hunt, P. W. Wilkens, U. Singh, A. J. Gijsman, and J. T. Ritchie (2003), The DSSAT cropping system model, *European Journal of Agronomy*, *18*235-265.

Kimball, J. S., S. W. Running, and S. S. Saatchi (1999), Sensitivity of boreal forest regional water flux and net primary production simulations to sub-grid-scale land cover complexity, *Journal of Geophysical Research-Atmospheres*, *104*,259BT-0043 259BT: Document Delivery available, 27789-27801.

Kucharik, C. J., and T. E. Twine (2007), Residue, respiration, and residuals: Evaluation of a dynamic agroecosystem model using eddy flux measurements and biometric data, *Agricultural and Forest Meteorology*, *146*,WOS:000250180400002, 134-158.

Kueppers, L., M. Snyder, and L. Sloan (2007), Irrigation cooling effect: Regional climate forcing by land-use change, *Geophysical Research Letters*, *34*Art. No. L03703.

Lai, C. T., W. Riley, C. Owensby, J. Ham, A. Schauer, and J. R. Ehleringer (2006), Seasonal and interannual variations of carbon and oxygen isotopes of respired CO_2 in a tallgrass prairie: Measurements and modeling results from 3 years with contrasting water availability, *Journal of Geophysical Research-Atmospheres*, *111*,ISI:000236730800003.

Law, B. E., E. Falge, L. Gu, D. D. Baldocchi, P. Bakwin, P. Berbigier, K. Davis, A. J. Dolman, M. Falk, J. D. Fuentes, A. Goldstein, A. Granier, A. Grelle, D. Hollinger, I. A. Janssens, P. Jarvis, N. O. Jensen, G. Katul, Y. Mahli, G. Matteucci, T. Meyers, R. Monson, W. Munger, W. Oechel, R. Olson, K. Pilegaard, K. T. Paw, H. Thorgeirsson, R. Valentini, S. Verma, T. Vesala, K. Wilson, and S. Wofsy (2002), Environmental controls over carbon dioxide and water vapor exchange of terrestrial vegetation, *Agricultural and Forest Meteorology*, *113*,WOS:000179188300007, 97-120.

Lenihan, J., R. Drapek, D. Bachelet, and R. Neilson (2003), Climate change effects on vegetation distribution, carbon, and fire in California, *Ecological Applications*, *13*1667-1681.

Li, F. Q., W. P. Kustas, M. C. Anderson, J. H. Prueger, and R. L. Scott (2008), Effect of remote sensing spatial resolution on interpreting tower-based flux observations, *Remote Sensing of Environment*, *112*,ISI:000253068100005, 337-349.

Lin, J., C. Gerbig, S. Wofsy, A. Andrews, B. Daube, C. Grainger, B. Stephens, P. Bakwin, and D. Hollinger (2004), Measuring fluxes of trace gases at regional scales by Lagrangian observations: Application to the CO_2 Budget and Rectification Airborne (COBRA) study, *Journal of Geophysical Reserach-Atmospheres*, *109*Art. No. D15304

Lokupitiya, R. S., D. Zupanski, A. S. Denning, S. R. Kawa, K. R. Gurney, and M. Zupanski (2008), Estimation of global CO2 fluxes at regional scale using the maximum likelihood ensemble filter, *Journal of Geophysical Research-Atmospheres*, *113*,ISI:000260393300001.

Moore, C. J. (1986), Frequency response corrections for eddy correlation systems, *Boundary Layer Meteorology*, *37*17-35.
Nemani, R. R., C. D. Keeling, H. Hashimoto, W. M. Jolly, S. C. Piper, C. J. Tucker, R. B. Myneni, and S. W. Running (2003), Climate-driven increases in global terrestrial net primary production from 1982 to 1999, *Science*, *300*,ISI:000183333100052, 1560-1563.
Parton, W. J., A. R. Mosier, and D. S. Schimel (1988), Dynamics of C, N, P, and S in grassland soils: a model., *Biogeochemistry*, *5*109-131.
Peters, W., A. R. Jacobson, C. Sweeney, A. E. Andrews, T. J. Conway, K. Masarie, J. B. Miller, L. M. P. Bruhwiler, G. Petron, A. I. Hirsch, D. E. J. Worthy, G. R. van der Werf, J. T. Randerson, P. O. Wennberg, M. C. Krol, and P. P. Tans (2007), An atmospheric perspective on North American carbon dioxide exchange: CarbonTracker, *Proceedings of the National Academy of Sciences of the United States of America*, *104*,ISI:000251498700012, 18925-18930.
Potter, C. S., J. T. Randerson, C. B. Field, P. A. Matson, P. M. Vitousek, H. A. Mooney, and S. A. Klooster (1993), Terrestrial ecosystem production: a process model based on global satellite and surface data, *Global Biogeochemical Cycles*, *7*811-842.
Prince, S. D., and S. N. Goward (1995), Global primary production: A remote sensing approach, *Journal of Biogeography*, *22*,ISI:A1995UK05300026, 815-835.
Raupach, M., G. Marland, P. Ciais, C. LeQuere, J. Canadell, G. Klepper, and C. Field (2007), Global and regional drivers of accelerating CO_2 emissions *Proc. of the National Academy of Sciences of the USA*, *104*10288-10293.
Riley, W. J., C. J. Still, M. S. Torn, and J. A. Berry (2002), A mechanistic model of $H_2{}^{18}O$ and $C^{18}OO$ fluxes between ecosystems and the atmosphere: Model description and sensitivity analyses, *Global Biogeochemical Cycles*, *16*1095-1109.
Riley, W. J., C. J. Still, B. R. Helliker, M. Ribas-Carbo, and J. A. Berry (2003), ^{18}O composition of CO_2 and H_2O ecosystem pools and fluxes in a tallgrass prairie: Simulations and comparisons to measurements, *Global Change Biology*, *9*,740DV-0005 740DV: Document Delivery available, 1567-1581.
Riley, W. J., J. T. Randerson, P. N. Foster, and T. J. Lueker (2005), The influence of terrestrial ecosystems and topography on coastal CO_2 measurements: A case study at Trinidad Head, California, *JGR-Biogeosciences*, *110*.
Rodenbeck, C., S. Houweling, M. Gloor, and M. Heimann (2003), Time-dependent atmospheric CO2 inversions based on interannually varying tracer transport, *Tellus Series B-Chemical and Physical Meteorology*, *55*,ISI:000182698400036, 488-497.
Running, S. W., and E. R. Hunt (1993), Generalization of a forest ecosystem process model for other biomes, BIOME-BGC, and an application for global-scale models, in *Scaling Physiological Processes: Leaf to Globe*, edited by J. R. Ehleringer and C. B. Field, pp. 141-158, Academic Press, San Diego.
Schuh, A. E., A. S. Denning, M. Uliasz, and K. D. Corbin (2009), Seeing the forest through the trees: Recovering large-scale carbon flux biases in the midst of small-scale variability, *Journal of Geophysical Research-Biogeosciences*, *114*,ISI:000269030200001.
Sellers, P. J., Y. Mintz, Y. C. Sud, and A. Dalcher (1986), A simple biosphere model (SiB) for use within general circulation models, *Journal of the Atmospheric Sciences*, *43*505-531.
Sellers, P. J., S. O. Los, C. J. Tucker, C. O. Justice, D. A. Dazlich, C. J. Collatz, and D. A. Randall (1996), A revised land surface parameterization (SiB2) for atmospheric GCMs. Part

II: The generation of global fields of terrestrial biophysical parameters from satellite data, *Journal of Climate*, *9*706-737.

Sellers, P. J., D. A. Randall, C. J. Collatz, J. A. Berry, C. B. Field, D. A. Dazlich, C. Zhang, and G. D. Colello (1996), A revised land surface parameterization (SiB2) for atmospheric GCMs. Part 1: Model formulation, *Journal of Climate*, *9*676-705.

Sellers, P. J., F. G. Hall, R. D. Kelly, A. Black, D. Baldocchi, J. Berry, M. Ryan, K. J. Ranson, P. M. Crill, D. P. Lettenmaier, H. Margolis, J. Cihlar, J. Newcomer, D. Fitzjarrald, P. G. Jarvis, S. T. Gower, D. Halliwell, D. Williams, B. Goodison, D. E. Wickland, and F. E. Guertin (1997), BOREAS in 1997: Experiment overview, scientific results, and future directions, *Journal of Geophysical Research*, *102*28,731-728,770.

Stephens, B., K. Gurney, P. Tans, C. Sweeney, W. Peters, L. Bruhwiler, P. Ciais, M. Ramonet, P. Bousquet, T. Nakazawa, S. Aoki, T. Machida, G. Inoue, N. Vinnichenko, J. Lloyd, A. Jordan, M. Heimann, O. Shibistova, R. Langenfelds, L. Steele, R. Francey, and A. Denning (2007), Weak northern and strong tropical land carbon uptake from vertical profiles of atmospheric CO_2, *Science*, *316*1732-1735.

Stern, N. (2006), Stern Review on the economics of climate change, Cambridge University Press, Cambridge, UK.

Still, C. J., J. A. Berry, M. Ribas-Carbo, B. R. Helliker, and S. B. Verma (2003), The contribution of C_3 and C_4 plants to the carbon cycle of a tallgrass prairie: an isotopic approach, *Oecologia*, *DOI: 10.1007/s00442-003-1274-8*.

Turner, D. P., W. B. Cohen, and R. E. Kennedy (2000), Alternative spatial resolutions and estimation of carbon flux over a managed forest landscape in Western Oregon, *Landscape Ecology*, *15*,ISI:000088036700004, 441-452.

Turner, D. P., S. Ollinger, M. L. Smith, O. Krankina, and M. Gregory (2004), Scaling net primary production to a MODIS footprint in support of Earth observing system product validation, *International Journal of Remote Sensing*, *25*,ISI:000220718500010, 1961-1979.

Turner, D. P., W. D. Ritts, W. B. Cohen, S. T. Gower, S. W. Running, M. S. Zhao, M. H. Costa, A. A. Kirschbaum, J. M. Ham, S. R. Saleska, and D. E. Ahl (2006), Evaluation of MODIS NPP and GPP products across multiple biomes, *Remote Sensing of Environment*, *102*,ISI:000238406000008, 282-292.

USDA (2002), The Census of Agriculture, edited, USDA.

Wang, W. G., K. J. Davis, B. D. Cook, C. X. Yi, M. P. Butler, D. M. Ricciuto, and P. S. Bakwin (2007), Estimating daytime CO2 fluxes over a mixed forest from tall tower mixing ratio measurements, *Journal of Geophysical Research-Atmospheres*, *112*,ISI:000246846400003.

Webb, E. K., G. I. Pearman, and R. Leuning (1980), Correction of flux measurements for density effects due to heat and water vapor transfer, *Quarterly Journal of the Royal Meteorological Society*, *106*85-100.

Williams, I., W. Riley, J. Berry, M. Torn, and M. Fischer (2005), Regional-Scale Surface CO_2 Exchange Estimates Using a Boundary Layer Budget Method Over the Southern Great Plains, paper presented at American Geophysical Union, San Francisco, CA, December 5-9.

Zhang, L., B. Wylie, T. Loveland, E. Fosnight, L. L. Tieszen, L. Ji, and T. Gilmanov (2007), Evaluation and comparison of gross primary production estimates for the Northern Great Plains grasslands, *Remote Sensing of Environment*, *106*,ISI:000243701500004, 173-189.

Zhao, M. S., F. A. Heinsch, R. R. Nemani, and S. W. Running (2005), Improvements of the MODIS terrestrial gross and net primary production global data set, *Remote Sensing of Environment*, *95*,ISI:000227994900003, 164-176.